

See discussions, stats, and author profiles for this publication at: <https://www.researchgate.net/publication/44619225>

Multiscale entropy-based approach to automated surface EMG classification of neuromuscular disorders

Article in *Medical & Biological Engineering* · August 2010

DOI: 10.1007/s11517-010-0629-7 · Source: PubMed

CITATIONS

51

READS

43

4 authors, including:



Prodromos Kaplanis

Nicosia General Hospital

30 PUBLICATIONS 211 CITATIONS

[SEE PROFILE](#)



C. S. Pattichis

University of Cyprus

431 PUBLICATIONS 5,663 CITATIONS

[SEE PROFILE](#)



Damjan Zazula

University of Maribor

186 PUBLICATIONS 1,505 CITATIONS

[SEE PROFILE](#)

Some of the authors of this publication are also working on these related projects:



Deployment of Generic Cross-Boarder eHealth Services in Cyprus [View project](#)



Linked 2 Safety [View project](#)

Multiscale entropy-based approach to automated surface EMG classification of neuromuscular disorders

Rok Istenič · Prodromos A. Kaplanis ·
Constantinos S. Pattichis · Damjan Zazula

Received: 7 October 2009 / Accepted: 13 April 2010 / Published online: 21 May 2010
© International Federation for Medical and Biological Engineering 2010

Abstract We introduce a novel method for an automatic classification of subjects to those with or without neuromuscular disorders. This method is based on multiscale entropy of recorded surface electromyograms (sEMGs) and support vector classification. The method was evaluated on a single-channel experimental sEMGs recorded from biceps brachii muscle of nine healthy subjects, nine subjects with muscular and nine subjects with neuronal disorders, at 10%, 30%, 50%, 70% and 100% of maximal voluntary contraction force. Leave-one-out cross-validation was performed, deploying binary (healthy/patient) and three-class classification (healthy/myopathic/neuropathic). In the case of binary classification, subjects were distinguished with 81.5% accuracy (77.8% sensitivity at 83.3% specificity). At three-class classification, the accuracy decreased to 70.4% (myopathies were recognized with a sensitivity of 55.6% at specificity 88.9%, neuropathies with a sensitivity of 66.7% at specificity 83.3%). The proposed method is suitable for fast and non-invasive discrimination of healthy and neuromuscular patient groups, but it fails to recognize the type of pathology.

Keywords Surface electromyogram · Neuromuscular disorders · Continuous wavelet transform · Entropy · Support vector classification

1 Introduction

Neuromuscular disorders are related to pathological changes in the structure of motor units (MU) and can be roughly divided into muscular (myopathies) and neuronal disorders (neuropathies). In muscular disorders, single muscle fibres are successively lost during the progress of the disease [1]. Other typical symptoms are increased fibre diameter variation, fibrosis, perifascicular atrophy and focal muscle-fibre necrosis [34]. In neuronal disorders, the neuronal part of the MU is affected and all the muscle fibres belonging to the affected MU can no longer be excited (denervation) [7]. In some cases reinnervation also occurs, where the nerve terminals belonging to the most adjacent muscle fibres reinnervate denervated muscle fibres, resulting in an enlargement of the remaining MUs [34].

Changes in the structure of the MU affect its electrical activity, therefore intramuscular electromyogram (iEMG) is commonly used diagnostic tool in clinical practice [1, 2, 8, 11, 16, 17]. Recently, attempts to use surface electromyogram (sEMG) have also been made [7, 9, 13–15, 22, 23, 30, 37]. However, pathological EMG patterns that are known in iEMG cannot be directly addressed by their sEMG counterparts [7, 10, 31]. For example, measuring an insertional activity of the needle and spontaneous activity occurring at the single fibre level can only be performed by iEMG [40]. On the other hand, although the activity of individual MUs can be recorded with both iEMG and sEMG, muscle fibre

R. Istenič (✉) · D. Zazula
Faculty of Electrical Engineering and Computer Science,
University of Maribor, Smetanova 17, SI-2000 Maribor,
Slovenia
e-mail: rok.istenic@uni-mb.si

P. A. Kaplanis
The Cyprus Institute of Neurology and Genetics,
P.O. Box 23462, CY-1683 Nicosia, Cyprus

C. S. Pattichis
Department of Computer Science, University of Cyprus,
P.O. Box 20537, CY-1678 Nicosia, Cyprus

conduction velocity (MFCV) can generally be measured from sEMG only.

Various sEMG techniques have been studied for the diagnosis of neuromuscular disorders, including conventional bipolar sEMG [13, 22], linear electrode array [15] and matrix electrode array (high-density sEMG) [9, 10, 14, 30, 32]. The model for simulation of pathological changes in sEMG was introduced in [7]. The most investigated sEMG parameters include MFCV [33, 38, 39], MU size [9, 32], frequency spectra [13, 15], sEMG amplitude [9, 22] and sEMG entropy [7, 14]. However, although some studies have demonstrated feasibility of the detection of neuromuscular diseases from sEMG [9, 14, 30], the reported classification accuracy typically ranges from 70% to 80%. For this reason, surface EMG is not widely accepted as a valid diagnostic tool in neuromuscular diagnostics.

The separately reported successes of the frequency-based classification of neuromuscular disorders [13] and entropy-based feature extraction [4, 18, 20] inspired us to develop a combined classification approach. However, instead of the commonly used frequency transform of sEMG, we resorted to time-scale representation [12, 26, 27, 35, 36]. Although it has already been applied to various electrophysiological signals for diagnosis of different pathologies, such as Parkinson's disease [5], cerebral palsy [21] and lower back pain [28], it has never been combined with the entropy measures to investigate the amplitude distributions at different dyadic scales.

In our approach, the entropy-based feature extraction was used. The rationale for this is that entropy is a natural measure of differences in the sEMG amplitude distributions, which depend directly on neuromuscular condition. Therefore, entropy can detect changes in sEMG distribution due to pathology.

The rest of the paper is organized as follows: Sect. 2 describes materials and methods, including experimental setup and our novel multiscale entropy approach. In Sect. 3, the experimental results are presented, followed by a discussion in Sect. 4.

2 Materials and methods

2.1 Subjects

Twenty-seven subjects participated in the experiment: nine healthy volunteers (six males, three females), aged (mean \pm std. deviation) 53.7 ± 13.7 years; nine patients with muscular (seven males, two females), aged 52.8 ± 6.3 years; and nine patients with neuronal disorders (four males, five females), aged 50.6 ± 14.9 years. An attempt was made to keep the groups equal with respect to

age and gender, but no true matching procedure was applied.

The group of healthy volunteers consisted of subjects that have never been diagnosed with neuromuscular disease before and reported no significant neuromuscular disorders. In both groups of neuromuscular patients, the disease was diagnosed by an experienced neurologist prior to the measurement session. In the group of neuronal patients, six subjects had severe problems with arms. The affection of other three patients was not so severe, as their main problem was muscle weakness. Four out of nine myopathic patients were affected severely; three of them were recovering from a severe myopathy, whereas two of them had been suffering from the myopathy for a longer period.

2.2 Experimental set-up

Surface EMG of dominant biceps brachii (BB) muscle was acquired by a four-bar silver electrode with an interelectrode distance of 10 mm and a bar width of 1 mm (Dispositivi Elettronici Medicali, Italy) and amplified by the Nicolet Viking IV, two-channel EMG amplifier unit with the 20–500 Hz bandwidth (12 dB/octave). The recording system was connected to a specially designed force measurement system, which was placed at the foot end of the bed and was designed for monitoring the different contraction levels. Contraction forces were displayed in a real time on an oscilloscope as a graphical feedback to the subject. The force measurement strap, placed around the wrist of the subject, was connected to the system through a custom-made force transducer. A personal computer was connected to the EMG unit for storing raw sEMG, digitized by a 12-bit Analogue-to-Digital (A/D) converter (National Instruments) with the sampling frequency of 1 kHz.

2.3 Experimental protocol

Subjects laid on the bed, face up, with their dominant arm placed along the body and elbow abducted at 90° (180° corresponds to full elbow extension). Special care was taken to reduce the co-activation of other muscles. Thus, it was ensured that the dominant arm was not lifted from the bed or moved away from the body [29].

Before the electrode placement, the length of the BB muscle was measured with the elbow abducted at 90° and the skin was cleaned with alcohol. Conductive paste was applied on the electrodes and the electrode array was placed over the BB, with the second electrode (in proximal–distal direction) at a distance equal to $1/3$ of the total BB length. This arrangement ensured that all four electrodes were between the innervation zone and the tendon.

The ground electrode was placed on the dominant wrist and four surface electrodes were connected in a single differential configuration (SD), so two channels were recorded per each session (1st channel: electrodes 1 and 2, 2nd channel: electrodes 3 and 4).

First, each subject performed 5-s long maximum voluntary contraction (MVC) three times with 2 min of rest in between. A target contraction level of the average MVC was marked on the oscilloscope. After 2 min of rest the subject contracted the BB muscle up to the target contraction level displayed on the oscilloscope. Once the exerted force stabilized, 5 s of the sEMG were recorded, followed by 2 min of rest. The same procedure was repeated twice for each contraction level. Then, the target level was changed to 70%, 50%, 30% and 10% of MVC and the process was repeated.

2.4 Feature extraction using multiscale entropy

The recorded signals were visually inspected for the presence of artefacts, such as inadequate skin–electrode contacts, excessive noise, non-existence of MU action potentials (MUAPs), etc. In a limited number of pathology cases, one out of two recorded channels had to be discarded. Thus, for consistency reasons, better of the two channels recorded per subject was chosen for further analysis also in the cases with two good sEMG channels. Frequency spectrum of each signal was also inspected and the power line interference (50 Hz and its higher harmonics) was suppressed using an off-line spectral interpolation [25]. Examples of preprocessed signals are depicted in Fig. 1.

Preprocessed signals were transformed into time-scale representation using continuous wavelet transform (CWT) [35]. Denote the sEMG by $s(t)$ and the mother wavelet by $\psi(t)$. The transformed sEMG at a scale $a > 0$ and translation b was obtained as:

$$S_w(a, b) = \frac{1}{\sqrt{a}} \int_{-\infty}^{+\infty} s(t) \overline{\psi\left(\frac{t-b}{a}\right)} dt \quad (1)$$

where $\bar{\psi}(t)$ is the complex conjugate of the mother wavelet $\psi(t)$, $b = 0, \dots, N-1$ stands for its translation in time, and N is the length of $s(t)$ (in samples). In our experiment, the Haar wavelet was empirically chosen. Besides the Haar wavelet, we experimented also with other types of mother wavelets, such as Daubechies, Morlet and Mexican hat. Each sEMG channel was transformed to 8 dyadic scales $a = 2^i$, $i = 1, \dots, 8$. The pseudo-frequencies of Haar wavelet corresponding to each scale from 2 to 256 are: 498, 249, 124, 62, 31, 16, 8 and 4 Hz, respectively. An example

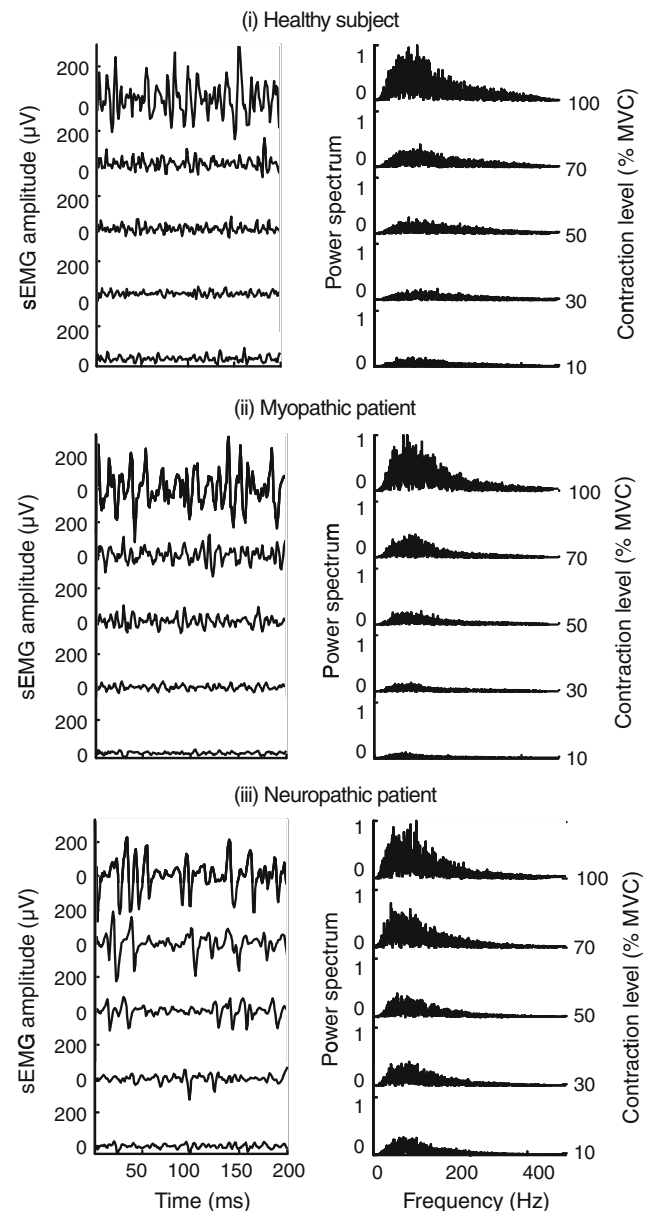


Fig. 1 Time (left) and frequency (right) representation of sEMG of (i) healthy subject, (ii) myopathic patient and (iii) neuropathic patient at all five contraction levels studied; y-axis labels amplitudes and contraction levels, while x-axis labels time and frequency, respectively. Power spectrum is normalized by its maximal value over all the contraction levels

of sEMG time-scale representation for healthy subject at 50% MVC is depicted in Fig. 2.

Next, the Shannon entropy of the transformed sEMG $S_w(a, b)$ was computed at each dyadic scale and over all possible translations $b = 0, \dots, N-1$:

$$\begin{aligned} H_a &= H(S_w(a, b)) \\ &= - \sum_{i=1}^M P(S_w(a, b) = s_i) \log_2 P(S_w(a, b) = s_i) \end{aligned} \quad (2)$$

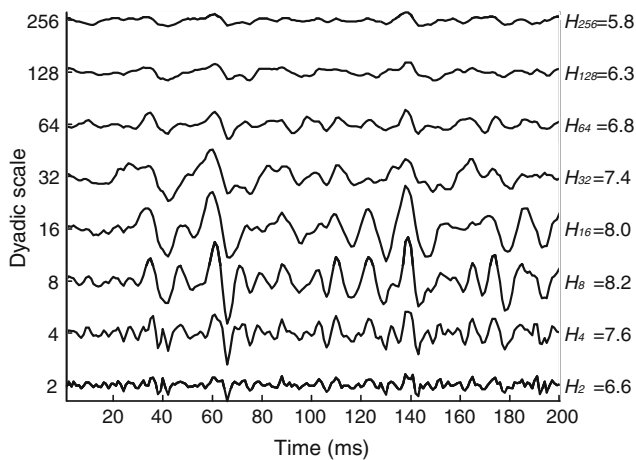


Fig. 2 Time-scale representation of a sEMG of healthy subject at 50% MVC transformed by Haar wavelet to 8 dyadic scales. x -axis labels time, left y -axis scale of the wavelet transform, while entropy scored at each scale is reported on the right-hand side of the plot. For example $H_2 = 6.6$ means that entropy of the transformed sEMG at the scale 2 is 6.6

where H_a stands for the entropy at scale a , and $S_w(a, b)$ is considered a realization of a discrete ergodic random process, occupying the value s_i with probability $P(S_w(a, b) = s_i)$, $i = 1, \dots, M$. The values of $S_w(a, b)$ were partitioned into M partitions ($M = 1000$) of maximal peak-to-peak amplitude interval over all the contraction levels per subject, and the probability $P(S_w(a, b) = s_i)$ was determined by the number of samples in each partition.

Because the range of entropic values depends on the number of partitions, the choice of the interval partitioning is decisive. When comparing the entropy of different signals, the interval should be fixed for all signals. In case of fixed interval, the entropy depends on the amplitude and distribution of the signal. But sEMG amplitude depends on various factors and it varies among individual subjects. It has been reported that absolute comparisons of sEMG amplitude are not appropriate [6] and that sEMG amplitude should be normalized with respect to the reference contraction of a subject [19]. Thus, to compensate for inter-subject variability of sEMG amplitude, the interval was partitioned for each subject individually, but fixed for all contraction levels of one subject. In this way we achieved that entropy is a measure for the sparsity of the sEMG and less dependant on indeterminacies caused by sEMG amplitude. Besides the approach where interval is partitioned for each subject separately, we tried also fixed interval for all subjects. Although on our dataset there were no significant differences between two different types of partitioning on the performance of the method, we decided to support the compensation of sEMG amplitude in our manuscript. The result of the described feature extraction

technique was a vector of 40 entropies per subject (8 scales by 5 contraction levels).

2.5 Classification

C-Support vector classification (C-SVC) [3], implemented in LIBSVM package,¹ was used for the classification of extracted 40-dimensional feature vectors. C-SVC presumes l n -dimensional training vectors $\mathbf{x}_i \in R^n$, $i = 1, \dots, l$, belonging to two classes and a vector of class labels $\mathbf{y} \in R^l$ such that $y_i \in \{1, -1\}$ and solves the following optimization problem:

$$\min_{\alpha} \left(\frac{1}{2} \alpha^T Q \alpha - \mathbf{e}^T \alpha \right), \quad (3)$$

subject to $\mathbf{y}^T \alpha = 0$, where the i -th element of α is limited to $0 \leq \alpha_i \leq C$, $i = 1, \dots, l$, \mathbf{e} is a vector of ones, $C > 0$ is the upper bound, and Q is an $l \times l$ positive semidefinite matrix with (i, j) -th element defined as $Q_{ij} \equiv y_i y_j K(\mathbf{x}_i, \mathbf{x}_j)$. In our experiments, radial basis function $K(\mathbf{x}_i, \mathbf{x}_j) = e^{-\gamma \|\mathbf{x}_i - \mathbf{x}_j\|^2}$ was chosen as a kernel because it non-linearly maps instances into a higher dimensional space and can, therefore, handle the non-linear relation between class labels and attributes. The parameters $\gamma = 2^{-4}$ and $C = 2^{10}$ were defined empirically. Finally, the decision function was defined as:

$$f(\mathbf{x}) = \sum_{i=1}^l y_i \alpha_i K(\mathbf{x}_i, \mathbf{x}). \quad (4)$$

C-SVC was initially developed for binary classification problems, but can be generalized to multi-class problems by using the ‘one-against-one’ approach. This approach constructs $k(k-1)/2$ classifiers, where k is the number of classes. Each classifier is trained using data from two classes and voting strategy is used afterwards to find the winning class [3].

In our experiments, two datasets were created, one for the binary classification (healthy/patient) and the other for the three-class classification (healthy/myopathic/neuropathic). Each subject in the dataset was represented by a 40-dimensional vector of entropies and a class label. For testing purposes, each dataset was divided into 26 training and 1 testing subjects (the leave-one-out cross-validation technique). This procedure was then repeated 26-times, so that each subject was once used in the testing set. In each iteration, Eq. 3 was applied to train the classifier while the testing subject was classified according to Eq. 4. Finally, the classification accuracy, defined as the number of correctly classified versus the number of all subjects was computed.

¹ Software available at <http://www.csie.ntu.edu.tw/~cjlin/libsvm>.

3 Results

3.1 Classification of multiscale entropy

Mean values of the extracted multiscale entropies for healthy and patient groups for all scales and contraction levels are depicted in Fig. 3. ANOVA with Tukey's honestly significant difference test was used to test for significant differences between both groups. Considering only individual combinations of contraction level and scale, the differences in mean entropies of healthy and patient groups were insignificant. But when considering all contraction levels and all scales together, mean entropy in patient group was significantly lower than the mean entropy in healthy group ($P < 0.01$).

Deploying leave-one-out cross-validation on a dataset with a total of 27 subjects, classification accuracy was 81.5% (77.8% sensitivity, 83.3% specificity) for binary and 70.4% for three-class classification (myopathic disorders were recognized with a sensitivity of 55.6% at specificity 88.9%, neuropathic disorders with a sensitivity of 66.7% at specificity 83.3%). Figure 4 shows the receiver operating characteristic (ROC) of binary classification, illuminating the classification's trade-off between the true positive rate

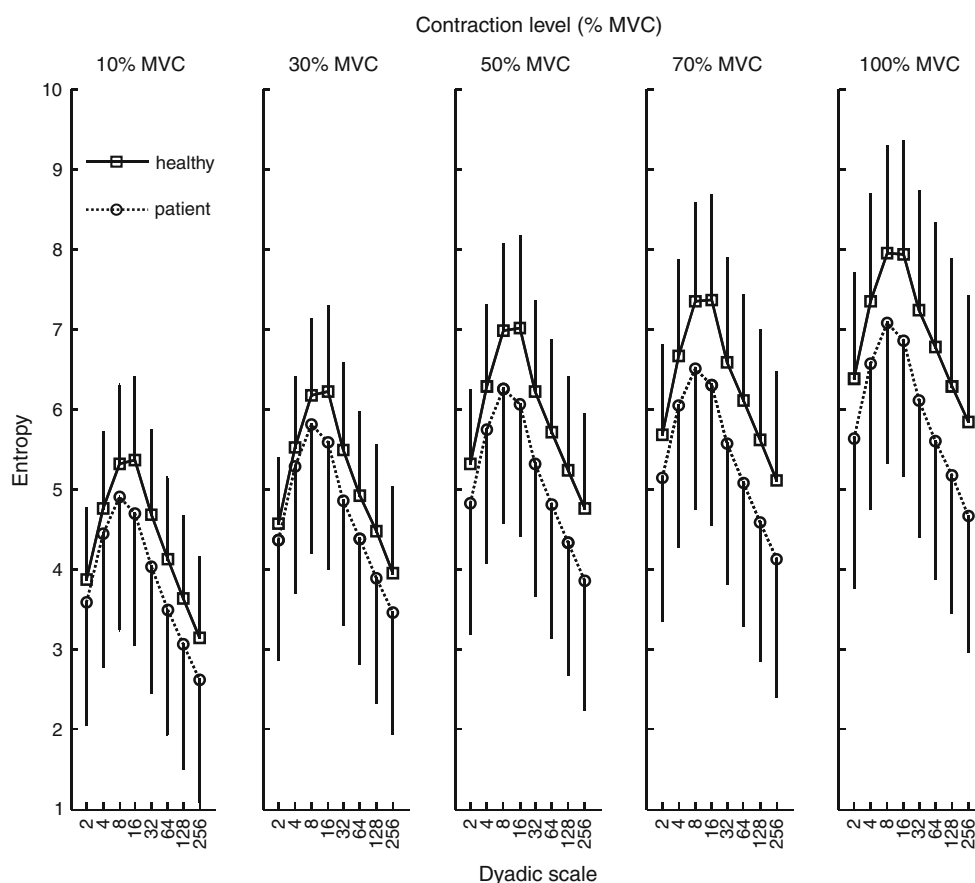
(the number of true positives divided by the number of all subjects), and the false positive rate (the number of false positives divided by the number of all subjects). In three-class classification the greatest problem was caused by the similarities of myopathic and neuropathic groups: three out of nine neuropathic and four out of nine myopathic patients were misclassified, whereas eight out of nine healthy subjects were classified correctly.

3.2 An effect of mother wavelet, scales and contraction levels on classification accuracy

Table 1 reports the obtained binary classification accuracy for the Haar, Daubechies (order 8), Morlet and Mexican hat mother wavelets. The highest accuracy was scored by the Haar mother wavelet, followed by Morlet, Daubechies 8 and Mexican hat. The superior performance of Haar wavelet was mainly due to the superior specificity (83.3% compared to the 77.8% for Morlet and Daubechies 8).

We further investigated sensitivity of our method to inclusion/exclusion of different contraction levels. In particular, the performance of binary classification with Haar wavelet was evaluated at each contraction level separately (10% MVC, 30% MVC, etc.). Out of all individual

Fig. 3 Mean values of the multiscale entropy for healthy (solid line with squares), and patient (dotted lines with circles) groups; entropy is depicted versus 8 scales (bottom x-axis) at each contraction level 10, 30, 50, 70 and 100% MVC (upper x-axis). For clarity, std. deviation bars are plotted only on one side of the mean, i.e. mean + std. deviation for healthy and mean – std. deviation for patient group



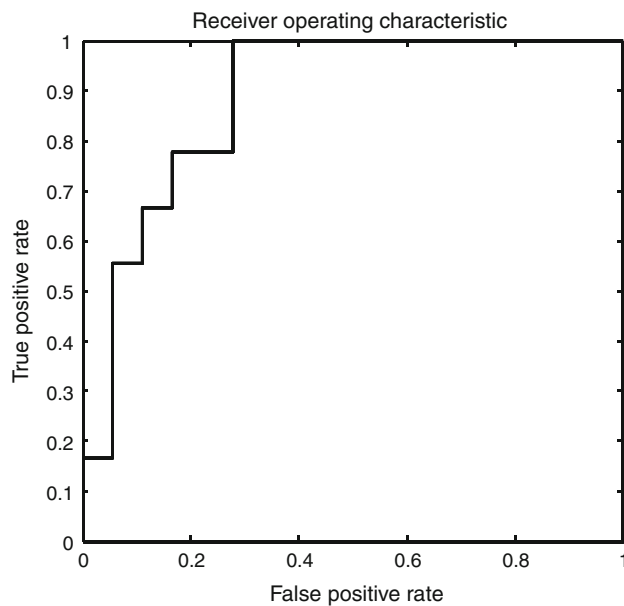


Fig. 4 The receiver operating characteristic for binary classification. Threshold values across the interval [0,1] were applied to the binary classifier outputs. For each threshold, two values were computed, the true positive ratio (the number of classifier outputs greater or equal to the threshold, divided by the number of true positives), and the false positive ratio (the number of outputs less than the threshold, divided by the number of false positives)

Table 1 Classification accuracy, sensitivity and specificity of multiscale entropy-based binary classification (healthy subjects versus patients) using different mother wavelets

Mother wavelet	Accuracy (%)	Sensitivity (%)	Specificity (%)
Haar	81.5	77.8	83.3
Morlet	77.8	77.8	77.8
Daubechies (order 8)	74.1	66.7	77.8
Mexican hat	74.1	77.8	72.2

contraction levels, the best classification accuracy was achieved at higher contraction levels (77.8% at 50% MVC, 74.1% at 70% MVC and 77.8% at 100% MVC), whereas significant drop of performance was observed when using low contraction levels (65% for 10% and 30% MVC). The best classification accuracy (81.5%) was achieved by combining all five contraction levels together, justifying the need for inclusion of the entire contraction range tested.

We also investigated the effect of inclusion/exclusion of different wavelet scales on the classification accuracy. Again, binary classification with Haar wavelet was performed, but this time only the entropies of a single scale at a time were taken into account for all five contraction levels. In addition, the complete leave-one-scale-out test was performed, ignoring one out of eight tested scales at a

time. No significant difference in classification accuracy was observed among different scales, whereas the best classification results were obtained when all the eight dyadic scales tested were included.

In order to justify the need for the multiscale entropy, we reclassified the signals by limiting the feature extraction stage to the entropy of raw sEMG only (without CWT). Mean values of extracted entropies are listed in Table 2. The classification accuracy decreased for 7.4% (from 81.5 to 74.1%) for binary classification, and for 7.5% (from 70.4% to 62.9%) for three-class classification, justifying the additional computational costs due to CWT analysis.

4 Discussion

A novel approach for an automatic classification of neuromuscular disorders has been developed, based on the multiscale entropy of sEMG. Surface EMG signal was first transformed to multiple scales by CWT. Entropy of transformed signals was used to reduce the complexity of feature space and classification was performed using obtained feature vectors.

Entropy depends on the amplitude distribution and measures the level of randomness on a predefined amplitude interval. Generally speaking, the closer the amplitude distribution to the uniform distribution on a predefined interval, the higher the entropy. This knowledge can be used to interpret the results of sEMG multiscale entropy, which, in healthy subjects, depends on at least three different parameters: the level of muscle contraction, wavelet scale and the distance between the active MU and the pick-up electrodes. Low contraction forces demand less MUAP triggering, which means sparser sEMG signals and, thus, lower entropy. By increasing contraction forces, number of activated MUs increases and the sEMG amplitudes distribute more normally over the amplitude range; therefore the entropy computes higher (Fig. 3). The entropy changes also with the wavelet scale; in our experiments it gradually increased up to the scale 8 (corresponding to pseudo-frequency of 124 Hz) at all force levels, and decreased with higher scales (Fig. 2). This is due to the progressive low-pass filtering of wavelet transform, because at higher scales, signals are smoother.

The entropy also depends on the density of sEMG interference pattern. According to the models of pathological iEMG [11] and sEMG [7], sEMG of healthy subjects should score the highest entropy, because the sEMG amplitudes are distributed more normally across the predefined range than in the presence of pathology. In myopathy muscle fibres in MUs are progressively lost. Consequently, when compared to healthy condition, the maximum amplitude of sEMG peaks is decreased [7].

Table 2 Entropy (mean \pm std. deviation) of raw sEMG (without CWT) for three groups of subjects (healthy, myopathic and neuropathic) and five contraction levels

Contraction level (% MVC)	Healthy group	Myopathic group	Neuropathic group
10	4.4 \pm 1.0	3.8 \pm 1.7	4.2 \pm 1.5
30	5.2 \pm 0.9	4.6 \pm 1.7	4.8 \pm 1.5
50	5.9 \pm 1.1	5.2 \pm 1.6	5.1 \pm 1.6
70	6.3 \pm 1.3	5.7 \pm 1.5	5.4 \pm 1.7
100	7.0 \pm 1.4	6.6 \pm 1.5	5.9 \pm 1.7
10–100	5.7 \pm 1.6	5.2 \pm 1.9	5.0 \pm 1.8

In the bottom, the average entropy value over all the contraction levels is reported

Therefore, sEMG amplitude distribution is concentrated closer around zero, and entropy is lower than in case of healthy subjects, especially at high contraction forces. Besides fibre loss, the MFCV variability is increased in myopathy, with significant decrease in MFCV reported in severe cases [11, 14, and references therein]. Because entropy increases with MFCV, myopathic sEMG should score lower entropy than normal sEMG.

In neuropathy, MUs are denervated and sEMG shows isolated peaks with little activity between two adjacent peaks [7], i.e. sEMG pattern becomes sparser. This results in decreased entropy. Another physiological change in neuropathy is reinnervation with common consequence, such as increased MUAP amplitude because of increased number of fibres in the enlarged MUs [32, 34]. Increase of MUAP amplitude reflects in wider sEMG amplitude distribution and, hence, increased entropy. But the increase in entropy due to reinnervation is smaller than its decrease due to denervation, because all denervated MU cannot become reinnervated [34]. Consequently, neuropathic sEMG should score lower entropy in comparison to normal.

Since the entropy is decreased in both pathologies, it is impossible for our method to differentiate between pathologies, because the differences are insignificant. When compared to surface electrodes, iEMG electrodes are more selective and enable sampling from nearby muscle fibres. Hence, iEMG signals are always relatively sparse and distinction between myopathy and neuropathy is typically based on MUAP shapes [2, 16, 17]. But also in iEMG there are features that are not capable of making the distinction between neuropathy and myopathy, such as MFCV [11, 38] and fibrillation potentials [11].

Our experimental findings agree very well with these theoretical assumptions; entropy of healthy group was always the highest, followed by myopathic and neuropathic groups (Table 2). Furthermore, except for the lowest contraction forces tested (10% and 30% MVC), the entropy of neuropathic sEMG was lower than the entropy of myopathic sEMG. On the other hand, the differences in the

multiscale entropy between myopathic and neuropathic groups were insignificant and the results of our three-class classification are not so promising, especially the sensitivities to myopathic (55.6%) and neuropathic (66.7%) conditions. This limitation is common to all existing sEMG techniques and can currently be surpassed only by the means of iEMG.

The results of our method are comparable to other similar sEMG-based studies. For example, Kaplanis et al. [15] reported classification approach based on five sEMG parameters: turns and zero crossings per second, median frequency, total power per second and bispectrum peak amplitude and the k-nearest neighbour classifier and demonstrated separation of healthy/patient groups with a success rate of 69%, Güler and Koçer [13] combined sEMG spectral analysis with PCA and reported the accuracy of 85%. Huppertz et al. [14] used the following parameters: MFCV, dwell time over root mean square, autocorrelation function, and chi-value, derived from high-density sEMG, and reported the classification accuracy of 81%. Slightly higher accuracy rates were demonstrated by techniques for classification of iEMG [2, 8, 16, 17, 27]. These techniques mainly consist of an automatic MUAP detection followed by the iEMG decomposition, and classification of the decomposed MUAPs. Katsis et al., for example, reported success rate of 86% [16] and 89% [17], Christodoulou and Pattichis 97% [2], and Pattichis and Pattichis 82% [27]. In all these cases, success rates decrease significantly when discrimination of neuropathic and myopathic patients is attempted.

The accuracy of our binary classification scored 81.5%. Although inferior to the classification rates of advanced iEMG techniques, the achieved classification accuracy was comparable to other published sEMG-based approaches [13–15]. Furthermore, its simplicity and low computational complexity make it an appealing candidate for non-invasive identification of neuromuscular disorders in patients, who do not tolerate the needles (e.g., children, professional athletes, etc.) or for long-term and repetitive monitoring of neuromuscular disorders.

Only the use of sEMG for the classification of neuromuscular patients was discussed so far. Besides sEMG, the force profiles could also be used for classification. Muscle weakness is typical for neuromuscular disorders. Because of the loss of muscle fibres (muscular disorders) or the loss of entire MUs (neuronal disorders) the neuromuscular patients are expected to reach lower maximal forces comparing to healthy subjects, however, generated forces depend on the severity of disease, gender, age and are subject to significant inter-subject variability. They should be compared very carefully.

Several limitations of our method should be mentioned. First, with only one muscle investigated per subject, the extent of myopathic/neuropathic changes is difficult to access. The method detects the differences in amplitude distributions that can vary also between subjects in the same group, depending on the stage of the disease, muscle strength and thickness of subcutaneous tissue. Although these factors can degrade the classification results, no significant differences in classification between the patients, recovering from the disease and the patients suffering from a severe disease were found in this study, as some members of both groups were misclassified. Finally, in this study, the number of sEMG channels was limited to one. Thus, the positioning of electrodes between tendon compliance and motor end-point became critical, requiring a skilled operator for sEMG acquisition. However, the method can easily be extended to high-density sEMG [10, 24, 30], replacing the manual electrode positioning step with automated post-selection of a few high quality sEMG channels.

In conclusion, our method is suitable for fast and non-invasive discrimination of healthy and neuromuscular patient groups, but fails to recognize the type of pathology itself. Nevertheless, a simple experimental protocol (only one pair of bipolar signals and relatively short acquisition time) and a low-computational complexity make our approach attractive tool for non-invasive diagnosis and assessment of the neuromuscular disease, especially when the use of the needles is either not recommended or not possible.

Acknowledgements This work was supported by the Slovenian Ministry of Higher Education, Science and Technology (Contract No. 1000-05-310083 and Programme Funding P2-0041) and bilateral Slovenian-Cypriot research project DePaSSE (Detection of pathological changes in sEMGs using statistical and entropy-based approaches).

References

1. Anand N, Chad D (2007) Electrophysiology of myopathy. In: Blum AS, Rutkove SB (eds) *The clinical neurophysiology primer*. Humana Press, New Jersey, pp 325–352
2. Christodoulou CI, Pattichis CS (1999) Unsupervised pattern recognition for the classification of EMG signals. *IEEE Trans Biomed Eng* 46:169–178
3. Cortes C, Vapnik V (1995) Support-vector networks. *Mach Learn* 20:273–297
4. Costa M, Goldberger AL, Peng CK (2005) Multiscale entropy analysis of biological signals. *Phys Rev E* 71(2):021906
5. De Michele G, Sello S, Carboncini MC, Rossi B, Strambi SK (2003) Cross-correlation time-frequency analysis for multiple EMG signals in Parkinson's disease: a wavelet approach. *Med Eng Phys* 25:361–369
6. Dimitrova NA, Dimitrov GV (2003) Interpretation of EMG changes with fatigue: facts, pitfalls, and fallacies. *J Electromyogr Kinesiol* 13:13–36
7. Disselhorst-Klug C, Silny J, Rau G (1998) Estimation of the relationship between the noninvasively detected activity of single motor units and their characteristic pathological changes by modelling. *J Electromyogr Kinesiol* 8:323–335
8. Dobrowolski A, Tomczykiewicz K, Komur P (2007) Spectral analysis of motor unit action potentials. *IEEE Trans Biomed Eng* 54:2300–2302
9. Drost G, Stegeman DF, Schillings ML, Horemans HLD, Janssen HMHA, Massa M, Nollet F, Zwartz MJ (2004) Motor unit characteristics in healthy subjects and those with postpoliomyelitis syndrome: a high-density surface EMG study. *Muscle Nerve* 30:269–276
10. Drost G, Stegeman DF, van Engelen BGM, Zwartz MJ (2006) Clinical applications of high-density surface EMG: a systematic review. *J Electromyogr Kinesiol* 16:586–602
11. Fuglsang-Frederiksen A (2006) The role of different EMG methods in evaluating myopathy. *Clin Neurophysiol* 117:1173–1189
12. Gazzoni M, Farina D, Merletti R (2004) A new method for the extraction and classification of single motor unit action potentials from surface EMG signals. *J Neurosci Methods* 136:165–177
13. Güler NF, Koçer S (2005) Classification of EMG signals using PCA and FFT. *J Med Syst* 29:241–250
14. Huppertz HJ, Disselhorst-Klug C, Silny J, Rau G, Heimann G (1997) Diagnostic yield of noninvasive high spatial resolution electromyography in neuromuscular diseases. *Muscle Nerve* 20:1360–1370
15. Kaplanis PA, Pattichis CS, Christodoulou CI, Hadjileontiadis LJ, Roberts CV, Kyriakides T (2004) A surface electromyography classification system. In: *IFMBE proceedings of 10th mediterranean conference on medical and biological engineering and computing and Health Telematics*, vol 6, pp 278–281
16. Katsis CD, Goletsis Y, Likas A, Fotiadis DI, Sarmas I (2006) A novel method for automated EMG decomposition and MUAP classification. *Artif Intell Med* 37:55–64
17. Katsis CD, Exarchos TP, Papaloukas C, Goletsis Y, Fotiadis DI, Sarmas I (2007) A two-stage method for MUAP classification based on EMG decomposition. *Comput Biol Med* 37:1232–1240
18. Kaufman M, Zurcher U, Sung PS (2007) Entropy of electromyography time series. *Physica A* 386:698–707
19. Keenan KG, Farina D, Maluf KS, Merletti R, Enoka RM (2005) Influence of amplitude cancellation on the simulated surface electromyogram. *J Appl Physiol* 98:120–131
20. Kosmidou VE, Hadjileontiadis LI (2009) Using sample entropy for automated sign language recognition on sEMG and accelerometer data. *Med Biol Eng Comput* 48(3):255–267
21. Lauer RT, Stackhouse CA, Shewokis PA, Smith BT, Tucker CA, McCarthy J (2007) A time-frequency based electromyographic analysis technique for use in cerebral palsy. *Gait Posture* 26:420–427
22. Lindeman E, Spaans F, Reulen JPH, Leffers P, Drukker J (1999) Surface EMG of proximal leg muscles in neuromuscular patients

- and in healthy controls. Relations to force and fatigue. *J Electromyogr Kinesiol* 9:299–307
23. Meekins GD, So Y, Quan D (2008) American association of neuromuscular and electrodiagnostic medicine evidenced-based review: use of surface electromyography in the diagnosis and study of neuromuscular disorders. *Muscle Nerve* 38:1219–1224
 24. Merletti R, Holobar A, Farina D (2008) Analysis of motor units with high-density surface electromyography. *J Electromyogr Kinesiol* 18:879–890
 25. Mewett DT, Reynold KJ, Nazeran H (2004) Reducing power line interference in digitized electromyogram recordings by spectrum interpolation. *Med Biol Eng Comput* 42(4):524–531
 26. Nielsen M, Kamavuako EN, Andersen MM, Lucas MF, Farina D (2006) Optimal wavelets for biomedical signal compression. *Med Biol Eng Comput* 44(7):561–568
 27. Pattichis CS, Pattichis MS (1999) Time-scale analysis of motor unit action potentials. *IEEE Trans Biomed Eng* 46:1320–1329
 28. Pope MH, Aleksiev A, Panagiotacopoulos ND, Lee JS, Wilder DG, Friesen K, Stielau W, Goel VK (2000) Evaluation of low back muscle surface EMG signals using wavelets. *Clin Biomech* 15:567–573
 29. Rainoldi A, Galardi G, Maderna L, Comi G, Lo Conte L, Merletti R (1999) Repeatability of surface EMG variables during voluntary isometric contractions of the biceps brachii muscle. *J Electromyogr Kinesiol* 9:105–119
 30. Rau G, Disselhorst-Klug C (1997) Principles of high-spatial-resolution surface EMG (HSR-EMG): single motor unit detection and application in the diagnosis of neuromuscular disorders. *J Electromyogr Kinesiol* 7:233–239
 31. Rau G, Schulte E, Disselhorst-Klug C (2004) From cell to movement: to what answers does EMG really contribute? *J Electromyogr Kinesiol* 14:611–617
 32. Roelleveld K, Sandberg A, Stålberg EV, Stegeman DF (1998) Motor unit size estimation of enlarged motor units with surface electromyography. *Muscle Nerve* 21:878–886
 33. Schillings ML, Kalkman JS, Janssen HMHA, van Engelen BGM, Bleijenberg G, Zwarts MJ (2007) Experienced and physiological fatigue in neuromuscular disorders. *Clin Neurophysiol* 118: 292–300
 34. Stalberg E, Karlsson L (2001) Simulation of EMG in pathological situations. *Clin Neurophysiol* 112:869–878
 35. Strang G, Nguyen T (1995) Wavelets and filter banks. Cambridge Press, Wellesley
 36. Wang G, Wang Z, Chen W, Zhuang J (2006) Classification of surface EMG signals using optimal wavelet packet method based on Davies-Bouldin criterion. *Med Biol Eng Comput* 44(10): 865–872
 37. Wimalaratna HS, Tooley MA, Churchill E, Preece AW, Morgan HM (2002) Quantitative surface EMG in the diagnosis of neuromuscular disorders. *Electromyogr Clin Neurophysiol* 42: 167–174
 38. Yaar I, Niles L (1992) Muscle fiber conduction velocity and mean power spectrum frequency in neuromuscular disorders and in fatigue. *Muscle Nerve* 15:780–787
 39. Zwarts MJ, Stegeman DF (2003) Multichannel surface EMG: basic aspects and clinical utility. *Muscle Nerve* 28:1–17
 40. Zwarts MJ, Drost G, Stegeman DF (2000) Recent progress in the diagnostic use of surface EMG for neurological diseases. *J Electromyogr Kinesiol* 10:287–291